RSC Advances

This is an *Accepted Manuscript*, which has been through the Royal Society of Chemistry peer review process and has been accepted for publication.

Accepted Manuscripts are published online shortly after acceptance, before technical editing, formatting and proof reading. Using this free service, authors can make their results available to the community, in citable form, before we publish the edited article. This *Accepted Manuscript* will be replaced by the edited, formatted and paginated article as soon as this is available.

You can find more information about *Accepted Manuscripts* in the Information for Authors.

Please note that technical editing may introduce minor changes to the text and/or graphics, which may alter content. The journal's standard Terms & Conditions and the Ethical guidelines still apply. In no event shall the Royal Society of Chemistry be held responsible for any errors or omissions in this *Accepted Manuscript* or any consequences arising from the use of any information it contains.

ROYAL SOCIETY OF CHEMISTRY

www.rsc.org/advances

A carbon ion beam irradiated MWCNT/AuNPs composite sensor for sensitive assay of purine-nucleosides of DNA

Pankaj Gupta, Rosy and Rajendra N Goyal*
Department of Chemistry, Indian Institute of Technology Roorkee, Roorkee-247667 (India)
E.Mail: rngcyfcy@iitr.ac.in, Tel: +911332-285794 (O)

Abstract

Multi-walled carbon nanotubes (MWCNT) and gold nanoparticles (AuNPs) composite modified glassy carbon (MWCNT/AuNPs/GC) was irradiated with high energy carbon ion beam and the surface morphology of the irradiated sensor was analysed using Raman spectroscopy, FE-SEM and Electrochemical Impedance Spectroscopy (EIS). The irradiated MWCNT/AuNPs/GC sensor has been applied for the electrochemical investigation of deoxyguanosine (dGuo) and deoxyadenosine (dAdo) by using square wave voltammetry and cyclic voltammetry. The irradiated sensor has been found to exhibit an excellent electrocatalytic activity, leading to an enhancement in the peak currents of dGuo and dAdo. The peak potentials also shifted to less positive potentials as compared to the unirradiated MWCNT/AuNPs/GC (pristine). The peak current of dGuo and dAdo was found to be linear in the range of 1–500 μM and the detection limit of 126 and 109 nM, respectively, were observed. The practical utility of the irradiated sensor has been demonstrated by the determination of dGuo and dAdo in the DNA samples extracted from herring sperm and MCF7 cell line (human breast cancer cells). Further, the carbon beam irradiated sensor displayed high sensitivity and reproducibility and has been found suitable in clinical diagnosis.

Keywords

Deoxyguanosine, Deoxyadenosine, Carbon beam irradiation, cancer cells, voltammetry

RSC Advances Accepted Manuscript

Introduction

Deoxyguanosine (dGuo) and deoxyadenosine (dAdo) are the purine-ribonucleosides present in deoxyribonucleic acid (DNA). dGuo is selectively toxic for adult T lymphocytes, hence, it has been used in the production of lymphocyte-depleted embryonic thymus rudiment. In the absence or lack of enzyme purine nucleoside phosphorylase only dGuo is cytotoxic and directly phosphorylates in S49 cells, which is associated with immunodeficiency disease [1-3]. dGuo can react with polyunsaturated fatty acids (PUFAs) in the lipid peroxidation under oxidative conditions, which promotes the formation of 8-hydroxydeoxyguanosine (8-OH- dGuo) [4]. This reaction may cause damages in the DNA structure, resulting in a disruption of the double helix structure and allowing the guanine sites to be more accessible. Oxidative DNA damage has been implicated in aging, carcinogenesis and other degenerative diseases. The urinary excretion of the DNA repair product 8-OH-dGuo has been proposed as a non-invasive biomarker of *in vivo* oxidative DNA damage in humans [5, 6]. Inherited deficiency in the enzyme adenosine deaminase (ADA) or purine-nucleoside phosphorylase has been associated with severe combined immunodeficiency. The elevated level of dGuo and adenosine in plasma is found to be toxic to proliferating mammalian cells, including lymphocytes [3,7]. The combination of dAdo and deoxycoformycin has been found to affect the growth of a human colon carcinoma cell line [8, 9]. It has also been reported that high concentration of dAdo inhibits DNA synthesis and cell division in animals and also contributes to the dialysis-induced immune deficiency [10]. dAdo has been used as a useful precursor in the synthesis of a wide variety of antiviral, antitumor and antileukemic drugs and has also exhibited a cardio protective action [11]. The pathological conditions of a patient have been found to affect the level of purine nucleosides and the corresponding purine bases in the body fluids. The abnormal level of purine

RSC Advances Accepted Manuscript

nucleosides excreted in the urine and serum has been shown to be related to carcinoma [12-14]. Both the deoxyribonucleosides of DNA are electroactive, therefore, the measurement of the concentration level of the nucleic bases and alterations in DNA composition can provide valuable insights into the genotoxicity, carcinogenesis, aging, and mutagenesis [15]. In view of the importance of dGuo and dAdo in human physiology, attempts have been made to simultaneously determine them in body fluids

Many techniques like high pressure liquid chromatography (HPLC), liquid chromatography/Mass spectrometry (LC/MS), fluorescence, micellar electrokinetic chromatography and capillary electrophoresis, etc. have been used to sense lesions in DNA and its oxidative damage [16-22]. Electrochemical techniques based on various approaches have also been developed for detecting the DNA damage with high selectivity and sensitivity. Electrochemical sensors provide a cost-effective, simple and ecofriendly approach to monitor DNA damages as they minimize the need for labeling the target nucleic acids and may provide information with spatial resolution. The electrochemical behaviour of nucleic acids and its purine bases has been reported earlier and the oxidation has been analyzed at different surfaces, including carbon, platinum, gold, silver, polymer etc. [15, 23, 24].

Last decade has seen an application of carbon nanotubes (CNT) in the surface modification of sensors to achieve higher sensitivity and selectivity. CNT are well-ordered, high aspect ratio allotropes of carbon, and have been receiving attention for their potential applications in future nanoelectronics, sensor designing, thin film electronics, detectors and other fields of materials science [25, 26]. The electronic and mechanical properties of CNTs are largely influenced through atomic scale defects and the defects can appear during the stage of CNT growth, purification and can be created by the chemical treatment to achieve the desired

RSC Advances Accepted Manuscript

functionality. Such imperfection in CNTs can also be introduced by irradiation, where, bombardment with energetic particles creates defects in the materials [27, 28]. The research on irradiation of carbon nanotubes with energetic particles is triggered by a broad range of new interesting phenomena, like coalescence and welding of nanotubes, surface reconstructions, change in mechanical properties and a decrease in the contact resistance between a carbon nanotube and metallic electrodes after the exposure of electron or ion beams [29, 30]. It is suggested that, when an energetic ion hits carbon-nanotube surface, the carbon atoms acquire kinetic energy and displace from their original positions and various atomic-scale defects such as vacancy defects in the walls or interstitial defect in the shells of CNTs are observed. The sputtering of carbon atoms has been found to produce the vacancies on the side walls and interstitial atoms and contribute to increase in the rough surface, reactivity and conductivity of nano tubes thin film [30-32]. Irradiation induced defects in the carbon nanostructure lattice leads to the extended reconstruction of sp^2 atomic network near the vacancies by the formation of dangling bonds and amorphous carbon inside the material. It has been observed that irradiation makes CNTs more conducting and reactive than unirradiated CNTs [27, 31]. A number of more complex defects from a purely hexagonal CNT network such as formation of coherent structure containing non-six-membered rings, formation of inter-shell covalent bond and pentagon/heptagon Stone-Wales defects associated with a rotation of a bond in the nanotube atomic network, give rise to the surface reconstruction and diameter reduction of CNTs. Thus, the morphology, size, hybridization and unique mechanical and electronic properties of carbon nanotubes can be suitably modified by the application of ion beam treatment. Integration of the gold nanoparticles (NPs) with carbon nanotubes (CNTs) has been explored for sensitive electrochemical determination because of the low resistance ohmic contacts of these composites.

RSC Advances Accepted Manuscript

The high active surface area-to-volume ratios and the synergistic electrocatalytic activity were achieved by combining gold nanoparticles with CNTs [33, 34]. Our particular interest in the nano-composites involving gold nanoparticles (AuNPs) is basically due to the fact that such a combination imparts unique electronic properties to CNTs along with the biocompatibility and electrocatalytic effects of AuNPs [35]. Simultaneous determination of dGuo and dAdo has great significance to bioscience and clinical diagnosis since both these compounds occur simultaneously in the body fluids. Intracellular levels of dGuo and dAdo are important, because their altered concentration stimulate metabolic disorders in human system. In view of the importance of purine nucleotides in human physiology and to know about its redox chemistry, various attempts have been made to analyse them in the body fluids by different techniques [23, 36-40]. Literature survey indicated that most of the studies reported on purine nucleosides deal with 8-hydroxy derivative of dAdo and dGuo. Some scarce attempts are made on the determination of dAdo and dGuo by using different techniques. Table 1 presents various techniques used for the individual determination of dAdo and dGuo. However, to the best of our knowledge there are no reports for the simultaneous determination of dGuo and dAdo using voltammetric or any other techniques.

In this paper, we have carried out irradiation of the multi-walled carbon nano tube and gold nano-particles composite modified glassy carbon (MWCNTs/AuNPs/GC) by high energy carbon ion beam for the simultaneous determination of dGuo and dAdo in human biological samples. It was found that the irradiated MWCNT/AuNPs/GCE shows an excellent electrocatalytic activity towards the oxidation of dGuo and dAdo. The response of the anodic peak current and the detection limit of dGuo and dAdo at irradiated MWCNT/AuNPs composite was observed better in comparison to the earlier reported papers on purine bases [40-46].

RSC Advances Accepted Manuscript

2. Experimental Section

2.1. Chemical and Reagents

Deoxyguanosine (dGuo), deoxyadenosine (dAdo), $HAuCl_4.3H_2O$, sodium citrate, $NaBH_4$, uric acid and xanthine were obtained from Sigma Aldrich (USA). MWCNT (~ 98%) were obtained from Bucky, USA and used for the modification without further purification. Phosphate buffers of ionic strength (1.0 M) were prepared by the reported method [47]. Degraded free acid Herring Sperm DNA was bought from Sisco Research Laboratories Ltd., Mumbai. DNA of the MCF7 cell line (human breast cancer cells) was extracted in the Biotechnology department of IIT Roorkee according to the reported protocol [48].

2.2. Instrumentation

The voltammetric experiments were performed using a computerized Epsilon EC-USB voltammetric analyzer (BAS, West Lafayette, USA). A single compartment three-electrode cell assembly with irradiated MWCNT/AuNPs/GC as the working electrode, Pt wire as the auxiliary electrode and an Ag/AgCl (3 M NaCl) (Model MF-2052 RB-5B) as a reference electrode was used. MWCNT/AuNPs modified GCE was irradiated with carbon ion beam using 15 UD Pelletron Accelerator at Inter University Accelerator Centre, New Delhi, India. The irradiated surface was characterized using Field Emission Scanning Electron Microscopy (FE-SEM, model; Zeiss ultra plus 55) and Raman spectroscopy (Renishawinvia Raman microscopy). Electrochemical impedance spectroscopy (EIS) was performed using a potentiostat (model; Versastat 3, PAR).

2.3. Irradiation of MWCNT/AuNPs/GC

A 0.7 $mgmL^{-1}$ suspension of MWCNT was prepared by dispersing in double distilled water and N,N-dimethyl formamide (1:9) using ultrasonic agitation. The colloidal gold

RSC Advances Accepted Manuscript

nanoparticles (AuNPs) solution having an average particle diameter less than 5 nM, was prepared according to the reported method [49]. Prior to the modification, the 1cm x 1cm piece of GCE was first polished using a paste of alumina powder (grade I) and ZnO on micro cloth pad until a mirror like finish surface was obtained. Then it was rinsed several times with distilled water. To find the optimum amount for surface modification, different volumes of MWCNT and AuNPs were casted on the surface of GCE and the peak current response for dGuo and dAdo was determined. Finally, the 20 µL aliquot of MWCNT and 20 µL AuNPs were selected as the optimum amount for the modification of GCE surface. Thus, initially 20 µL of MWCNT was casted onto the clean GCE surface and left overnight for drying. In the second step, 20 µL solution of the AuNPs was drop casted on the MWCNT layered GCE, followed by drying at room temperature. Now, MWCNT/AuNPs modified GC was irradiated using 15 UD Pelletron Accelerator. 120 MeV carbon ions beam with a beam current~0.5 pnA was used with ion dose of 1e12 ions cm^{-2} and the vacuum chamber was kept at a pressure of $\sim 5 \times 10^{-6}$ Torr. In order to prepare the sensor with irradiated MWCNT/AuNPs/GC piece, a copper strip was attached to make electrical connection and then the GC piece was wrapped by using Scotch tape. A hole of 3 mm diameter was pierced on the front side of Scotch tape to allow access of the test solution to the irradiated sensing surface.

2.4. Sample Preparation

The required amount of dGuo and dAdo (1 mM) were dissolved in the double-distilled water to prepare stock solutions. In order to prepare the desired concentration of analytes, the required volume of the stock solution was added to the electrolytic cell containing 2 ml of phosphate buffer solution and the total volume was made to 4 ml using double distilled water. Square wave voltammograms were then recorded at the optimized parameters: initial E: 0 mV,

RSC Advances Accepted Manuscript

final E: 1500 mV, square wave frequency (f): 15 Hz, square wave amplitude (Esw): 25 mV, potential step: 4 mV. Optimum conditions for cyclic voltammetry (CV) were initial (E): 0 mV, switching potential (E): 1500 mV, final (E): 0 mV and scan rate (v): 100 mV/s.

2.4.1. Real sample preparation

Herring Sperm DNA (5 mg) was dissolved in 10 mL of phosphate buffer (pH 7.2) and used for further investigation. DNA (24 µl) extracted from MCF7 cell line, having a concentration of 0.35 µgµL^{-1} was diluted to 10 mL using phosphate buffer (pH 7.2) and heated in a water bath at 80˚C for ~30 min.

3. Result and discussion

3.1 Effect of Irradiation

3.1.1 Raman spectroscopic studies

A typical Raman spectrum of irradiated MWCNT/AuNPs/GC surface exhibited first and second order Raman scattering mode. The first order Raman scattering mode, D-mode (disorder) was observed at ~1360 cm^{-1}, high energy G-mode (graphite) at 1580 cm^{-1} and second-order Raman scattering from D-band variation, G´ band was observed at ~2700 cm^{-1} as shown in the Fig. 1 [50]. The shifts or intensity changes of the peaks are generally used to study the defect formation (damage) in CNTs under energetic ion irradiation. The D-band involves scattering from disorders or amorphous sp^2 carbon, vacancies, impurities, kinks or from other defects, which breaks the basic symmetry of the CNT sheet. The intensity of D-band is proportional to the amount of disorder in the sample, and the ratio between the intensities of D band and the first-order graphite G band provides a parameter that can be used for quantifying sample purity. Whereas, I_D/I_G intensity ratio certainly depends on the number of layers under irradiation and increased by the decreasing the number of layers [50-52]. The Raman spectrum of irradiated

RSC Advances Accepted Manuscript

MWCNT/AuNPs/GC is presented by curve b in Fig. 1. Figure clearly demonstrates the increased intensity of Raman bands on exposing the MWCNT/AuNPs to 120 MeV Carbon beam irradiation. The increase in the intensity of D-band can be attributed to the cleavage of nanotubes, sputtering of nano composite, creation of defects and ordered-to-amorphous transition in the CNT system [53, 54]. The formation of covalent bond crosslinks between CNTs can also be induced by the ion beam irradiation [29, 31, 55]. The conductivity of irradiated MWCNT sheets is thus improved due to decrease in the thickness of nano composite layer. However, the increase in ion fluence to 1e13, caused more damage to MWCNT/AuNPs and the catalytic activity was found to decrease. Therefore, optimized fluence of 1e12 ions cm^{-2} has been used to irradiate the MWCNT/AuNPs/GC sensor, at which minimum damage to MWCNT occurs.

3.1.2 Impedance studies

The electrochemical impedance studies for the bare GCE, pristine and irradiated MWCNT/AuNPs/GC were carried out to determine the charge transfer resistance at these surfaces in 1:1 solution of 5 mM $K_3Fe(CN)_6$ and 0.1 M KCl in the frequency range of 0.1 to 100 kHz at a potential of 0.05 V. The value of charge transfer resistance (R_{ct}) was determined using Randle's equivalent circuit. The linear part of the curve is due to the diffusion process and represents Warburg resistance (Z_W). The results were found to fit best to a simple Randles equivalence circuit. Fig. 2 represents a comparison of Nyquist plots observed for the bare GCE, pristine and irradiated MWCNT/AuNPs/GC sensors. In all the three cases a semicircular pattern followed by a linear portion was observed. At bare and pristine MWCNT/AuNPs/GC sensors, the charge transfer resistance for $Fe[CN]_6^{3-/4-}$ redox process was observed as 3600 Ω and 1900 Ω, respectively (curve a and b). On exposing the MWCNT/AuNPs/GC composite to irradiation by 120 MeV Carbon ion beam, the diameter of the semicircle was decreased. The charge transfer

RSC Advances Accepted Manuscript

resistance also significantly decreased to about 780 Ω (curve c). This indicated that the charge transfer rate increased after employing the ion beam onto the MWCNT/AuNPs composite. The impedance data also validate the results observed from the Raman spectroscopy.

The surface morphology of the pristine and 120 MeV carbon beam irradiated MWCNT/AuNPs modified GCE was studied using FE-SEM. The typical images observed are shown in Fig. 3. At pristine surface MWCNT and nano gold particles were clearly seen (Fig. 3A). On the other hand in the carbon beam irradiated MWCNT/AuNPs/GC, nano tubes and gold nanoparticles were scattered and slightly destroyed probably due to the impact of irradiation in comparison to the pristine sensor (Fig. 3A). Thus, exposure of the high energy carbon ion beam leads to CNT's with shorter lengths in comparison to the pristine MWCNTs.

3.2. Cyclic Voltammetry

Cyclic voltammetry (CV) is a useful electroanalytical method for the qualitative analysis of redox process, evaluation of electron transfer kinetic and reversibility of the reaction. Therefore, the anodic voltammetric behavior of dGuo and dAdo was studied using CV. The CVs were recorded at irradiated MWCNT/AuNPs/GC at pH 7.2 using a sweep rate of 100 mV s^{-1}. A well-defined oxidation peak (I_a) was observed for dGuo (Ep~970 mV), when sweep was initiated in the positive direction. When the direction of sweep was reversed, an ill-defined reduction peak at~-698 mV (II_c) was observed as shown in Fig 4A. The oxidation peak Ia can be attributed to the oxidation of dGuo involving $4H^+$, $4e^-$ resulting in a diimine (II) by a mechanism similar to that proposed for Guanosine [36]. The diimine (II) being unstable is attacked by a water molecule as shown in Scheme 1 to give an imine alcohol (III) [36]. In the reverse sweep, the imine alcohol is expected to undergo $2H^+$, $2e^-$ reduction to give imine alcohol (IV) responsible for the appearance of cathodic peak (II_c) [36, 37]. dAdo exhibited practically similar

RSC Advances Accepted Manuscript

voltammetric behaviour as observed for dGuo. Thus, a well-defined oxidation peak ($I_{a'}$) at Ep (1260 mV) was noticed in the CV for dAdo when sweep was initiated in the positive direction and a reduction peaks at~-730 mV ($II_{c'}$) was observed when the direction of sweep was reversed (Fig. 4A(b)). The appearance of peak $II_{c'}$ is due to the reduction of the species generated in peak $I_{a'}$. The electro-oxidation of dAdo in an overall $6H^+$, $6e^-$ reaction has been reported earlier [11] to give imine alcohol species.

A CV of a mixture of 100 μM dGuo and dAdo at the pristine and irradiated MWCNT/AuNPs/GC surfaces exhibited well-defined oxidation peaks for dGuo and dAdo. However, the peak potential shifted to more positive potentials at pristine with a marked decrease in the peak current. These results clearly reveal that the irradiated MWCNT/AuNPs composite GCE promotes the kinetics of the electrochemical oxidation of both dGuo and dAdo. To elucidate the nature of the electrode reaction, sweep rate studies were performed in the range 5-150 mVs^{-1}. For both the compounds, the peak current was found to increase with increase in sweep rates. The linearity of i_p versus v and i_p versus log(v) can be expressed by the following equations:

For dGuo:

$i_p(\mu A) = 0.1359\ v - 0.1873$ $(R^2 = 0.9961)$ ....(1)

$\log i_p = 0.8465 \log v - 0.5643$ $(R^2 = 0.9918)$ .....(2)

For dAdo:

$i_p(\mu A) = 0.1097\ v - 0.8203$ $(R^2 = 0.9991)$ .....(3)

$\log i_p = 0.7854 \log v - 0.5011$ $(R^2 = 0.9952)$ .....(4)

from the linearity of i_p versus v and log i_p versus log v (slope > 0.5), it was concluded that the oxidation of both the deoxy compounds involves adsorption complications.

RSC Advances Accepted Manuscript

3.3 Square wave voltammetry

The square wave voltammograms (SWVs) of dGuo and dAdo at pristine and irradiated MWCNT/AuNPs/GC were recorded using the optimized parameters of SWV. The SWVs obtained at pristine (a) and irradiated MWCNT/AuNPs/GC (b) for 100 μM dGuo and dAdo at pH 7.2 are presented in Fig. 5. It can be seen that dGuo exhibited a sharp oxidation peak with much enhanced peak current using irradiated sensor (Ep ~ 940 mV) as compared to the small peak at pristine (Ep ~ 1000 mV). Similarly in the case of dAdo, a small peak was observed at pristine at a peak potential (Ep ~ 1320 mV) as shown in Fig. 5B, while at irradiated sensor, a well-defined oxidation peak was observed at 1255 mV, with a significant increase in the current response. The square wave voltammograms of a mixture of dGuo and dAdo were also recorded at pristine and irradiated MWCNT/AuNPs/GC sensors as shown in Fig 5C. In this case two well-defined peaks were noticed corresponding to dGuo (~ 940 mV) and dAdo (~ 1255 mV). In another experiment the square wave voltammograms for a mixture of guanine, dGuo, adenine, and dAdo were recorded at irradiated MWCNT/AuNPs/GC sensors and it was found that four well-defined oxidation peaks (Ep~ 790 mV, 940 mV, 1080 mV and 1255) were observed. The peaks were found to be due to the oxidation of guanine, dGuo, adenine and dAdo respectively. These results indicate that irradiation by carbon ion beam induced defects in the nanostructure lattice and hence, accelerate the rate of electron transfer and catalyze the electro-oxidation of dGuo and dAdo by increasing the peak current and shifting the peak potential (Ep) to less positive potentials.

3.3.1. Electrochemical investigations of dGuo

The quantitative determination of dGuo was carried out at carbon ion beam irradiated MWCNT/AuNPs/GC. The square wave voltammograms were recorded for various concentration

RSC Advances Accepted Manuscript

of dGuo and it was found that the anodic peak current of dGuo increased with increase in the concentration of dGuo (Fig. 6A). The peak current (i_p) was linearly dependent on the concentration of dGuo in the range 1-500 μM. The values of the anodic peak current were obtained by subtracting the background current of the buffer solution and an average of at least three replicate measurements was used to plot the calibration curve. The linear relation of the peak current with dGuo concentration can be represented by the equation:

i_p (μA) = 0.0537 C + 2.4509 .....(5)

having a correlation coefficient of 0.988, where i_p is the peak current in μA and C is the concentration of dGuo in μM. The sensitivity of the proposed method was found to be 0.0537 μA μM^{-1}. The detection limit (LOD) and limit of quantification were determined using the relation 3σ/b and 10 σ/b respectively, where σ is the standard deviation of the blank solution and b is the slope of the calibration curve, and were found to be 126 nM and 420 nM, respectively.

The effect of pH on the oxidation potential of dGuo was studied in the pH range 2.20-10.0. It was observed that the Ep shifted towards less positive potentials with the increase in pH. The dependence of the peak potential on the pH of supporting electrolyte can be presented by the equation:

E_p (pH 2.20-10) = [-48.31 pH + 1280.7] V vs. Ag/AgCl ….(6)

having a correlation coefficient 0.998.

The dependence of the peak current of dGuo on the square wave frequency was studied in the frequency range 5–40 Hz using irradiated MWCNT/AuNPs/GC. The peak current of dGuo was found to increase linearly with increasing square wave frequency in the range 5–40 Hz indicating adsorption controlled nature of the electron transfer process. The dependence of the

RSC Advances Accepted Manuscript

peak current (i_p) on square wave frequency (f) was linear and the dependence can be described by the equation:

i_p (μA) = 0.3476f (Hz) +1.028 …..(7)

having a correlation coefficient of 0.994. The above results were further confirmed by the log plot analysis and the relation between log (i_p) vs log (f) can be represented as:

log (i_p) = 0.8851 log(f) - 0.2423 ....(8)

having a correlation coefficient 0.998. The slope value (>0.5) of log i_p vs. log v plot further confirmed that the oxidation of dGuo proceeds by an adsorption controlled pathway, which is in agreement with the results obtained using cyclic voltammetry.

3.3.2. Electrochemical investigations of dAdo

The effect of pH on the Ep of dAdo was similarly studied in the pH range 2.20–10.0 using irradiated MWCNT/AuNPs/GC sensor. The peak potential was dependent on pH and shifted to less positive potentials with increase in pH. The variation of E_p with pH can be expressed by the relation:

E_p (pH 2.20-10.0) = [-50.93 pH + 1624] V vs. Ag/AgCl ……..(9)

with a correlation coefficient of 0.984. The value of dE_p/dpH was close to 59 mV/pH and hence indicated that equal number of protons and electrons were involved in the oxidation. The effect of square wave frequency on the anodic peak current of dAdo was then studied by varying the frequency in the range 5-40 Hz at pH 7.2. The peak current of dAdo was found to increase linearly with increasing square wave frequency. The linear relation observed for peak current vs. f can be expressed by the equation:

i_p (μA) = 0.3348f (Hz) + 3.0929 ……(10)

having a correlation coefficient of 0.990. The plot between log i_p vs log f was also found to be linear and can be represented by the equation:

RSC Advances Accepted Manuscript

$\log (i_p) = 0.6568 \log(f) + 0.1534$ .....(11)

having a correlation coefficient 0.999. The slope value of log i_p vs. log f plot (>0.5), further confirmed that the nature of the electrode reaction was adsorption controlled.

Square wave voltammograms of dAdo at different concentrations were similarly recorded. The peak current (i_p) of the oxidation peak (after correction of background current) increased with the increase in concentration of dAdo at pH 7.2 as depicted in Fig. 6B. The i_p vs conc. plot was linear in the range 1 - 500 μM with a correlation coefficient of 0.993. The linear regression equation can be presented as:

$i_p\,(\mu A) = 0.0606\, C + 1.735$ .....(12)

where C is the concentration of dAdo having a sensitivity of 0.0606 μA μM^{-1}. The LOD and limit of quantification of dAdo were found to be 109 and 366 nM respectively.

3.3.3. Simultaneous determination of dGuo and dAdo

High levels of dGuo and dAdo in the blood serum of patients with inherited deficiency of either adenosine deaminase or purine-nucleoside phosphorylase have been reported in the literature [3, 7]. The high levels claimed are responsible for the associated immunological disorders and interference in DNA synthesis. Thus, the alteration in the concentration level of these deoxyribonucleosides or in DNA composition can help in the early diagnosis of oxidative DNA damage or other diseases like cancer. Hence, simultaneous determination of the two deoxynucleosides was attempted on the irradiated sensor. Fig. 7A shows square wave voltammograms for different concentrations of dGuo in the range of 15–150 μM when the concentration of dAdo was kept at constant concentration (50 μM). It was noticed that the anodic peak current of dGuo increased with an increase in its concentration, whereas, the peak current of dAdo remained practically unaffected. Similarly, Fig. 7B shows square wave voltammograms

RSC Advances Accepted Manuscript

obtained at increasing concentrations of dAdo in the range of 15-250 μM keeping the concentration of dGuo constant 50 μM. It was found that in this case the peak current for dAdo increased linearly with increasing concentration without affecting the peak current and peak shape of dGuo. The dependence of i_p on concentration in each case followed the same relation as observed in their individual determination. Hence, it was concluded that both analytes did not interfere with each other and thus, the proposed sensor can be successfully used for the simultaneous quantitative determination of dGuo and dAdo.

3.4. Interference study

The influence of the compounds commonly present in the blood and urine was studied as potential interfering substances, as they can interfere with the oxidation of dGuo and dAdo. Thus, the interference due to ascorbic acid (AA), uric acid (UA) and xanthine (XA) was studied by carrying out the analysis of 100 μM of dGuo and dAdo in the presence of these interferents. The concentration of the interferents was increased up to 20 fold excess under the optimized experimental conditions. Fig. 8A presents the effect of high concentration of potential interfering substances (UA and XA) on the voltammograms. It is clear from the voltammogram that UA and XA have no influence on the peak current and peak potential response of dGuo and dAdo. As AA was oxidized at -100 mV, hence, its presence even at 100 fold excess did not interfere in the determination of dGuo and dAdo. The SWVs were also recorded for a mixture of dGuo, thymine, dAdo and cytosine at irradiated MWCNT/AuNPs/GC sensor. In this case, four well-defined oxidation peaks (Ep~940 mV, 1130 mV, 1255 mV and 1400 mV) were observed. The peaks were found to be due to the oxidation of dGuo, thymine, dAdo and cytosine respectively. Thus, the peaks corresponding to thymine and cytosine were sufficiently apart from the peaks of dAdo and dGuo and did not interfere. Further, the interference of nucleobases guanine, adenine,

RSC Advances Accepted Manuscript

thymine and cytosine was examined on the determination of dGuo and dAdo. It was observed that adenine and thymine interfere with each other and a peak in the region 1110 -1130 mV was noticed for both the compounds, nevertheless, they did not show any noticeable effect on the voltammetric responses of dGuo and dAdo as has been shown in Fig 9. From the observed results, it was inferred that the irradiated sensor can be safely applied for the simultaneous determination of dGuo and dAdo in the biological fluids, urine and serum without facing difficulty even if common interfering species present.

3.5. Stability and Reproducibility

The stability of the irradiated MWCNT/AuNPs/GC sensor was evaluated by measuring the peak current response of fixed concentration of dGuo and dAdo at pH 7.2 over a period of 30 days. The sensor was used daily and stored at the room temperature of 22 ± 2º C. The results showed that for the first 10 days, the decrease in the peak current was insignificant having R.S.D. (1.16 % for dGuo) and (0.97 % for dAdo), suggesting thereby that the irradiated sensor had an excellent stability. After 10 days, the value of the peak current decreased and R.S.D. increased to >2.5%.

The reproducibility of the irradiated sensor has also been investigated. The intra-day precision of the method was evaluated by repeating six experiments in the solution containing 50 µM of dGuo and 50 µM of dAdo using the same irradiated MWCNT/AuNPs/GC. The R.S.D. value for the peak current was found to be 0.93% and 0.72% respectively for dGuo and dAdo, indicating an excellent reproducibility of the irradiated sensor. Further, sensor to sensor variation was investigated by measuring the current response of the six irradiated MWCNT/AuNPs/GC sensors for the same concentration of dGuo and dAdo. The respective RSD for these analytes

RSC Advances Accepted Manuscript

were found to be 1.47% and 1.04% respectively. Thus, it is concluded that the irradiated sensor has good reproducibility and stability.

3.6. Analytical applicability

3.6.1 Analysis of DNA

The carbon beam irradiated MWCNT/AuNPs/GC sensor was applied for the quantification of dGuo and dAdo content in DNA extracted from herring sperm DNA. Square wave voltammograms were recorded to analyse the contents in the solution of herring sperm DNA prepared as described in Section 2.4. It was found that four well separated peaks corresponding to the oxidation of uric acid (~275 mV), xanthine (~700 mV), dGuo (~946 mV) and dAdo (~ 1245 mV) were observed. To confirm the peaks of dGuo and dAdo, the sample were spiked with exogenous dGuo and dAdo and SWVs were recorded (Fig. 8B). By using standard addition plot the concentration of dGuo and dAdo in herring sperm DNA sample were detected as 29.94 and 20.67 μM, respectively. The recoveries of dGuo and dAdo were determined in the range of 98.19–101.10% and 99.25-100.41% respectively, as summarized in **SI Table** 1.

The DNA solution obtained from the MCF7 cell line was also analysed using same procedure and the concentration of dGuo and dAdo were detected as 28.13 and 9.15 μM, respectively. The solution was also spiked with known amount of dGuo and dAdo and recoveries were found in the range of 99.11–101.04% and 98.78-101.07% for dGuo and dAdo, respectively (**SI** Table 2).

4. Conclusion

A novel electrochemical sensor based on irradiation of MWCNT/AuNPs composite by high energy carbon ion beam has been developed for the determination of dGuo and dAdo.

RSC Advances Accepted Manuscript

Irradiation breaks the basic symmetry of nano-composite and introduces localized defects including amorphization in MWCNT sheets. The high energy carbon ion beam irradiated MWCNT/AuNPs/GC sensor exhibited strong synergistic electrocatalytic effects towards the oxidation of dGuo and dAdo. The fabricated sensor was successfully applied for the simultaneous determination of dGuo and dAdo in test and real samples (DNA material) using square wave voltammetry. Results obtained using the proposed protocol confirmed the good accuracy and precision of the proposed method. A linear relationship between the analytes concentration and the current response were obtained at irradiated MWCNT/AuNPs/GC sensor with excellent reproducibility and low detection limit of 126 and 109 nM for dGuo and dAdo, respectively. A comparison of the detection of the proposed voltammetric method with recently reported strategies for dGuo and dAdo by different methods [11, 15,38, 56-59] is presented in Table 1. The simultaneous analysis of dGuo and dAdo was successfully carried out and no interference due to the matrix complexity was observed. Thus, the irradiated MWCNT/AuNPs/GC can be successfully used for the determination of dGuo and dAdo in the field of clinical and biomedical diagnosis. Further efforts are in progress to study this sensor for monitoring oxidative DNA damage and a broad spectrum of genetic-related diseases and conditions.

Acknowledgment

Authors are thankful to the Director, Inter University Accelerator Center, New Delhi for permitting irradiation experiments and to Dr. Fouran Singh, Scientist F, Inter University Accelerator Center, New Delhi for the helpful discussions. Two of the authors (PG and Rosy) are thankful to the Ministry of Human Resources Development, New Delhi for awarding Senior Research Fellowship.

RSC Advances Accepted Manuscript

Reference

1. L. J. Gudas, B. Ullman, A. Cohen and D. W. Martin, *Cell*, 1978, **14**, 531-538.
2. E. J. Jenkinson, L. L. Franchi, R. K. and J. J. T. Owen, *Eur. J. Immunol.*, 1982, **12**, 583-587.
3. Y. Dahbo and S. Eriksson, *Eur. J. Biochem*., 1985, **150**, 429-434.
4. Y. Higuchi, *Arch. Biochem. Biophys.*, 2001, **392**, 65–70.
5. S. Loft, A. F. Nielsen, I. B. Jeding, K. Vistisen and H. Enghusen, *J. Toxicol. Environ. Health*, 1993, **40**, 391-404.
6. S. Loft, K. Vistisen, M. Ewertz, A. Tjanneland, K. Overvad and H. Enghusen, *Cardnogeoesis*, 1992, **13**, 2241-2247.
7. T. Sato and T. S. Chan, *J. Cell. Physiol.*, 1996, **166**, 288-295.
8. F. Giorgelli, M. Giannecchini, V. Bemi, G. Turchi, F. Sgarrella, M. G. Tozzi, and M. Camici, *J. Cell. Biochem.*, 2000, **80**, 241–247.
9. V. Bemi, N. Tazzini, S. Banditelli, F. Giorgelli, R. Pesi, G. Turchi, A. Mattana, F. Sgarrella, M. G. Tozzi and M. Camici, *Int. J. Cancer*, 1998, **75,** 713–720.
10. J. Sampol, B. Dussol, E. Fenouillet, C. Capo, J. l. Mege, G. Halimi, G. Bechis, P. Brunet, H. Rochat, Y. Berland and R. Guieu, *J. Am. Soc. Nephrol.*, 2001, **12**, 1721–1728.
11. R. N. Goyal and A. Dhawan, *Bioelectrochemistry*, 2006, **69**, 223-233.
12. A. Mugweru and J. F. Rusling, *Anal. Chem.*, 2002**, 74**, 4044-4049.
13. L. J. Marnett, *Carcinogenesis*, 2000, **21**, 361-370.
14. L. Z. Luo, K. M. Werner, S. M. Gollin and W. S. Saunders, *Mutat. Res.*, 2004, **554**, 375–385.
15. T. R. L. C. Paixao, C. C. M. Garcia, M. H. G. Medeiros and M. Bertotti, *Anal. Chem.*, 2007, **79**, 5392 5398.
16. H. J. Helbock, K. B. Beckman, M. K. Shigenaga, P. B. Walter, A. A. Woodall, H. C. Yeo and B. N. Ames, *Proc. Natl. Acad. Sci. USA,* 1998, **95**, 288–293.
17. P. Jaruga, H. Rodriguez and M. Dizdaroglu, *Free Radical Biol. Med.*, 2001, **31**, 336–344.
18. A. Weimann, D. Belling and H. E. Poulsen, *Nucleic Acids Res.*, 2002, **30**, 1-8.
19. A. V. Willems D. L. Deforce, C. H. V. Peteghem and J. F. V. Bocxlaer, *Electrophoresis*, 2005, **26**, 1221–1253.
20. P. Tuma, E. Samcova and V. Kvasnicova *J. Chromatogr., B*, 2004, **813**, 255–261.

RSC Advances Accepted Manuscript

21. W. Wang, L. Zhou, S. Wang, Z. Luo and Z. Hu, *Talanta*, 2008, **74**, 1050–1055.
22. P. Iadarola, G. Cetta, M. Luisetti, L. Annovazzi, B. Casado, J. Baraniuk, C. Zanone and S. Viglio, *Electrophoresis*, 2005, **26**, 752–766.
23. R.N.Goyal and S.P.Singh, *Carbon*, 2008, **46**, 1556-1562.
24. A.A. Ensafi, M. Amini and B. Rezaei, *Sens. Actuat. B,* 2013, **177**, 862-870.
25. H. Lord and S. O. Kelley, *J. Mater. Chem.*, 2009, **19**, 3127-3134.
26. C. Gao, Z. Guo, J. H. Liu and X. J. Huang, *Nanoscale*, 2012, **4**, 1948-1963.
27. P. G. Collins, *Oxford Handbook of Nanoscience and Technology: Frontiers and Advances,* A.V. Narlikar, & Y.Y. Fu, Eds. (Oxford Univ. Press, Oxford, 2009).
28. A. V. Krasheninnikov, K. Nordlund, M. Sirvio, E. Salonen and J. Keinonen, *Phys. Rev. B*, 2001, **63**, 245405.
29. A. Ishaq, Z. Ni, L. Yan, J. Gong, D. Zhu, *Radiat. Phys. Chem.*, 2010, **79**, 687–691.
30. A. V. Krasheninnikov, K. Nordlund and J. Keinonen, *Phys. Rev. B*, 2002, **65**, 165423.
31. A. V. Krasheninnikov and F. Banhart, *Nat. Mater.*, 2007, **6**, 725-733.
32. M. Sammalkorpi, A. Krasheninnikov, A. Kuronen, K. Nordlund and K. Kaski, *Phys. Rev.* B, 2004, **70**, 245416.
33. Y. Guo, S. Guo, Y. Fang, S. Dong, *Electrochim. Acta*, 2010, **55**, 3927–3931.
34. K. A. Mahmoud, S. Hrapovic and J. H. T. Luong, *Nano*, 2008, **2**, 1051-1057.
35. R. N. Goyal, S. Bishnoi, H. Chasta, M.. A. Aziz and M. Oyama, *Talanta*, 2011, **85**, 2626-2631.
36. R. N. Goyal, S. M. Sondhi and A. M. Lahoti, *New J. Chem.*, 2005, **29**, 587–595.
37. R. N. Goyal and G. Dryhurst, *J. Elecroanal. Chem.,* 1982, **135**, 75-91.
38. R. N. Goyal, S. Chatterjee and S. Bishnoi, *Electroanalysis*, 2009, **21**, 1369-1378.
39. W. Sun, Y. Li, Y. Duan and K. Jiao, *Biosens. Bioelectron.*, 2008, **24**, 988-993.
40. H. Yina, Y. Zhou, Q. Ma, S. Ai, Q. Chen and L. Zhu, *Talanta*, 2010, **82**,1193–1199.
41. K. Huang, D. Niu, J. Sun, C. Han, Z. Wu, Y. Li and X. Xiong, *Colloids Surf. B Biointerfaces*, 2011, **82**, 543-549.
42. H. Yin, Y. Zhou, Q. Ma, S. Ai, P. Ju, L. Zhu and L. Lu, *Process Biochem.*, 2010, **45**, 1707-1712.
43. R. N. Goyal, V. K. Gupta, M. Oyama and N. Bachheti, *Talanta*, 2007, **71**, 1110-1117.
44. R. N. Goyal, M. Oyama and A. Tyagi, *Anal. Chim. Acta*, 2007, **581**, 32-36.

RSC Advances Accepted Manuscript

45. W. Sun, Y. Duan, Y. Li, T. Zhan and K. Jiao, *Electroanalysis*, 2009, **21**, 2667-2673.
46. R. N. Goyal and A. Sangal, *J. Electroanal. Chem.*, 2003, **557**, 147-155.
47. G. D. Christian and W. C. Purdy, *J. Electroanal. Chem.*, 1962, **3**, 363-397.
48. K. Nikhil, S. Sharan, A. Chakraborty, N. Bodipati, R.K. Peddinti and P. Roy, *Exp. Cell. Res.,* 2014, **320**, 311-328.
49. P. Gupta, R. N. Goyal and Y. B. Shim, *Sens. Actuators, B*, 2015, **213**, 72–81.
50. L. Bokobza and J. Zhang, *eXPRESS Polym. Lett.*, 2012, **6**, 601–608.
51. A. Aitkaliyeva, M. S. Martin, T. A. Harriman, D. S. Hildebrand, D. A. Lucca, J. Wang, D. Chen and L. Shao, *Phys. Rev. B*, 2014, **89**, 235-437.
52. G. Compagnini, G. Forte, F. Giannazzo, V. Raineri, A. Magna and I. Deretzis, *J. Mol. Struct.*, 2011, **993**, 506-509.
53. O. Lehtinen, T. Nikitin, A. V. Krasheninnikov, L. Sun, F. Banhart, L. Khriachtchev and J. Keinonen, *New J. Phys.*, 2011, **13**, 1-19.
54. M. Tachibana, Characterization of laser-induced defects and modification in carbon nanotubes by Raman spectroscopy, *Physical and Chemical Properties of Carbon Nanotubes*, http://dx.doi.org/10.5772/52091.
55. A. Ishaq, L. Yan and D. Zhu, *Nucl. Instrum. Methods Phys. Res., Sect. B*, 2009, **267**, 1779–1782.
56. T. R.L.C. Paixao and M. Bertotti, *Electrochim. Acta*, 2007, **52**, 2181-2188.
57. E.A.C. Westberg, R. Singh, U. Hedebrant, G. Koukouves, V. L. Souliotis, P. B. Farmer, D. Segerback, S. Kyrtopoulos and M. Å. Törnqvist, *Toxicol. Lett.*, 2015, **232**, 28-36.
58. T. Gustavsson, A. Sharonov, D. Onidas and D. Markovitsi, *Chem. Phys. Lett.*, 2002, **356**, 49-54.
59. T. Yamamoto ,Y. Moriwaki, S. Takahashi, T. Fujita, Z. Tsutsumi, J. Yamakita, K. Shimizu, M. Shioda , S. Ohta and K. Higashino, *J. Chromatogr. B*, 1998, **719**, 55-61.

RSC Advances Accepted Manuscript

Table 1: A comparison of the previously reported strategies for the detection of dGuo and dAdo with the present method.

Electrode	Technique	Linear range (μM)	LOD (nM)	Real sample analysis	Reference
dGuo					
PGE	CSV & CPE	-----	-----	No	[11]
GC/RuOHCF	FIA	3.8 - 252	94	Calf thymus DNA	[15]
GC/RuOHCF	RDEV	-----	234	No	[56]
-	LC/MS	2.2 - 35	-----	DNA	[57]
Irradiated MWCNT/AuNPs/GC	SWV	1 -500	126	Herring sperm & MCF-7 cell line	This work
dAdo					
C_{60}-fullerene/GCE	SWV	0.01 - 100	80	Urine	[38]
-	FUS	-----	-----	No	[58]
-	HPLC	Upto 42	0.05	urine	[59]
Irradiated MWCNT/AuNPs/GC	SWV	1 -500	109	Herring sperm & MCF-7 cell line	This work

FIA - flow injection analysis, CSV & CPE - cyclic sweep voltammetry & controlled potential electrolysis, RDEV - rotating disc electrode voltammetry, FUS - fluorescence upconversion spectroscopy, RuOHCF - Ruthenium Oxide Hexacyanoferrate

RSC Advances Accepted Manuscript

Figure Captions

Scheme-1: A tentative mechanism proposed for the redox reactions of deoxyguanosine.

Fig. 1: A comparison of Raman spectra observed for (a) pristine and (b) 120 MeV carbon ion beam irradiated MWCNT/AuNPs/GC at a fluence of 1e12 ions cm^{-2}.

Fig. 2: Nyquist plots observed for electrochemical impedance measurements (a) GCE (b) pristine MWCNT/AuNPs/GC (c) Irradiated MWCNT/AuNPs/GC. The inset represents the Randle's equivalent circuit used for data fitting.

Fig. 3 Comparative FE-SEM images observed for (A) pristine MWCNT/AuNPs/GC and (B) Irradiated MWCNT/AuNPs/GC.

Fig. 4: [A] CVs of dGuo and dAdo recorded in a larger potential window at Irradiated MWCNT/AuNPs/GC in phosphate buffer of pH 7.2 at a scan rate of 100 mV s^{-1}. [B] A comparison of CVs recorded at (a) pristine and (b) Irradiated MWCNT/AuNPs/GC. The background is shown by dotted line.

Fig. 5: A comparative square wave voltammograms recorded for 100 μM dGuo and dAdo using (a) pristine and (b) carbon ion irradiated MWCNT/AuNPs/GC in pH 7.2 phosphate buffer. The background is shown by dotted line.

Fig. 6: (A) SWVs observed for the increasing concentration of dGuo using irradiated MWCNT/AuNPs/GC. Curves were recorded at (a) 1 (b) 5; (c) 10; (d) 20; (e) 30; (f) 50; (g) 100; (h) 150 (i) 200, (j) 300 and (k) 500 μM in phosphate buffer of pH 7.2; (B) SWVs recorded for increasing the concentrations of dAdo. Curves were recorded at (a) 1; (b) 10; (c) 20; (d) 30; (e) 50; (f) 100; (g) 150; (h) 200; (i) 300; (j) 500 μM concentrations using irradiated MWCNT/AuNPs/GC in phosphate buffer of pH 7.20; inset is the calibration plot.

RSC Advances Accepted Manuscript

Fig. 7 Square wave voltammograms of a mixture of dGuo and dAdo recorded at irradiated MWCNT/AuNPs/GC in phosphate buffer of pH 7.2. (A) At a fixed concentration of dAdo (50 μM) with increasing concentrations of dGuo (a) 15; (b) 30; (c) 50; (d) 100 and (e) 150 μM. (B) dAdo concentrations (a) 15; (b) 50; (c) 100; (d) 50; (e) 175 and (f) 250 μM at fixed concentration of dGuo (50 μM).

Fig. 8: (A) SWVs showing interference of uric acid (UA) and xanthine (XA) at fixed dGuo and dAdo concentration (100 μM). (B) SWVs showing herring sperm DNA (a) without any spiking, (b) with 30 μM dGuo + 40 μM dAdo, (c) with 50 μM dGuo + 80 μM dAdo, (d) with 80 μM dGuo + 120 μM dAdo and (e) 100 μM dGuo + 160 μM dAdo.

Fig 9: Typical voltammograms showing interference of guanine, adenine, thymine and cytosine at fixed dGuo and dAdo concentration (100 μM). The dotted line presents the background current.

RSC Advances Accepted Manuscript

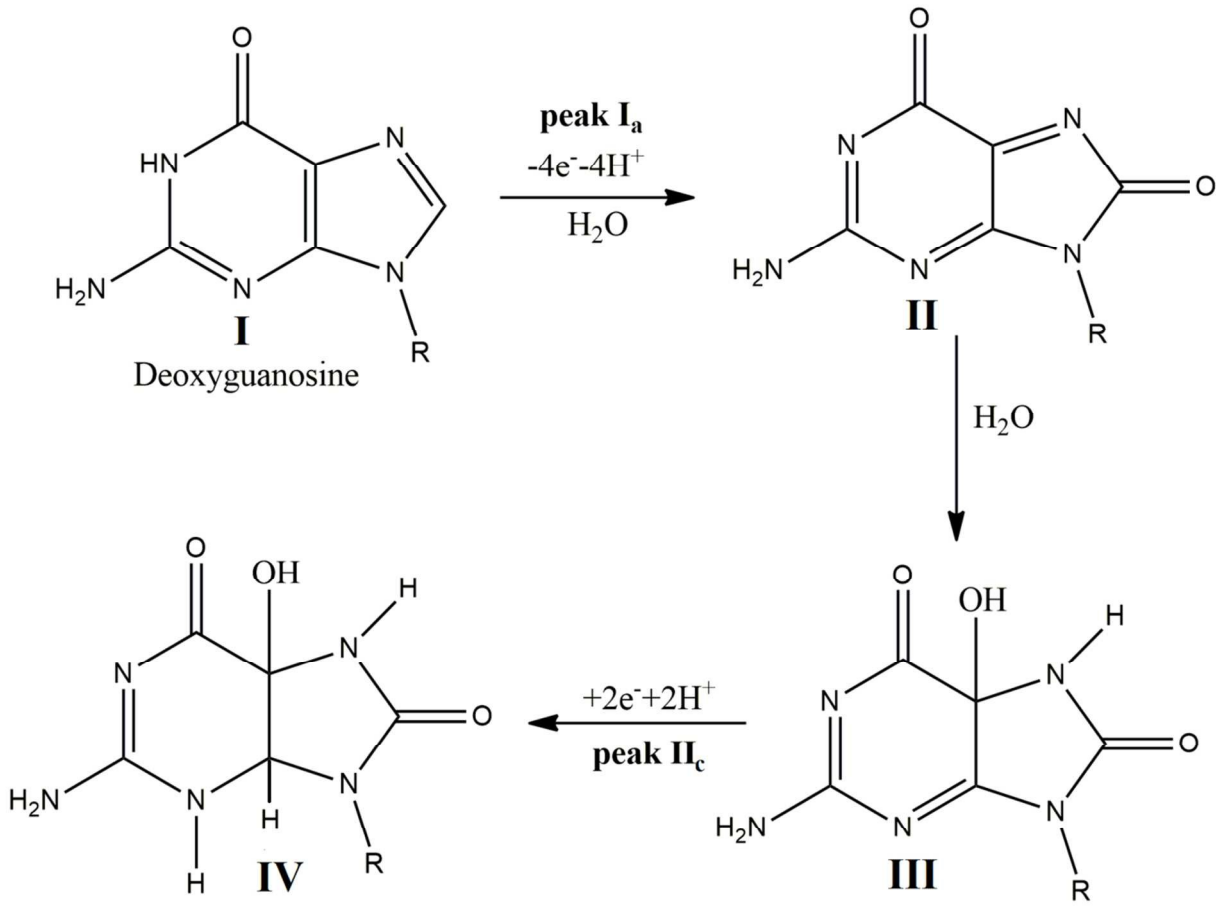

Scheme-1

RSC Advances Accepted Manuscript

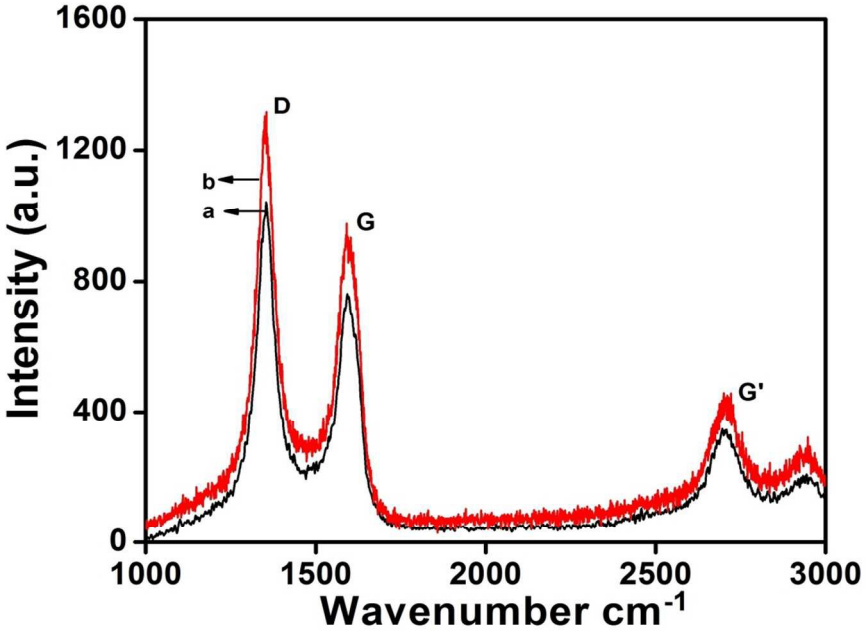

Fig. 1

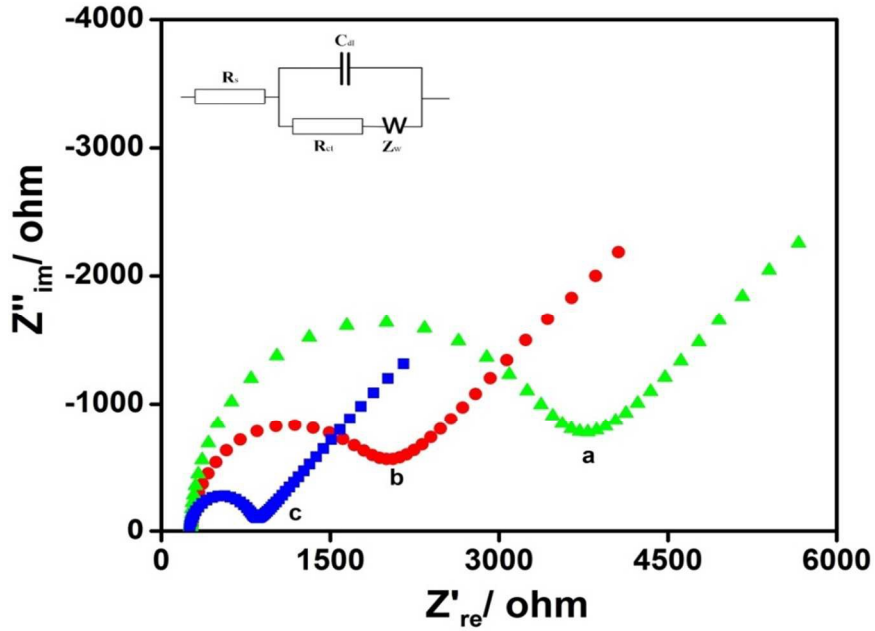

Fig. 2

RSC Advances Accepted Manuscript

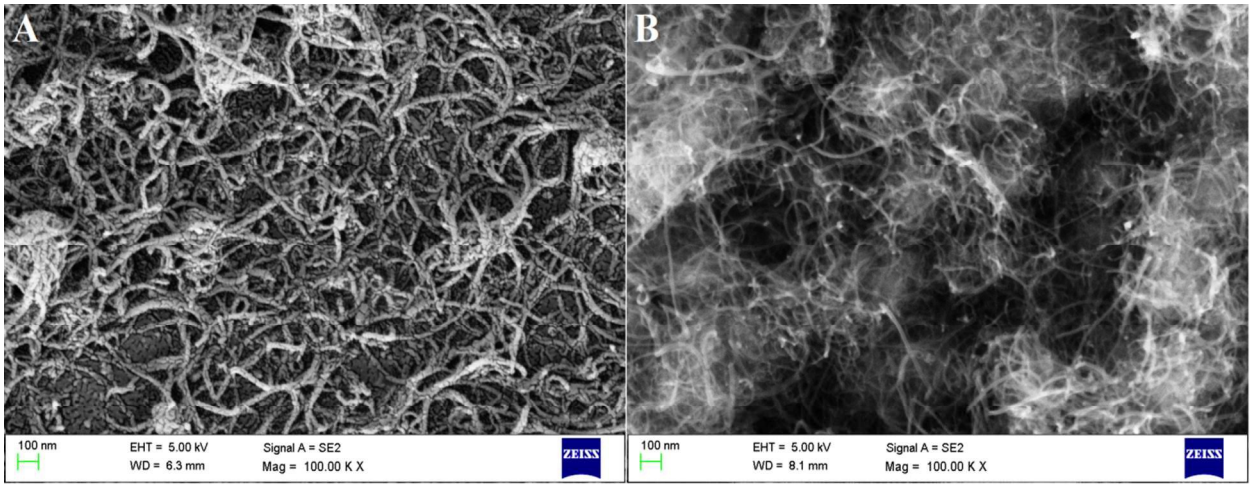

Fig. 3

RSC Advances Accepted Manuscript

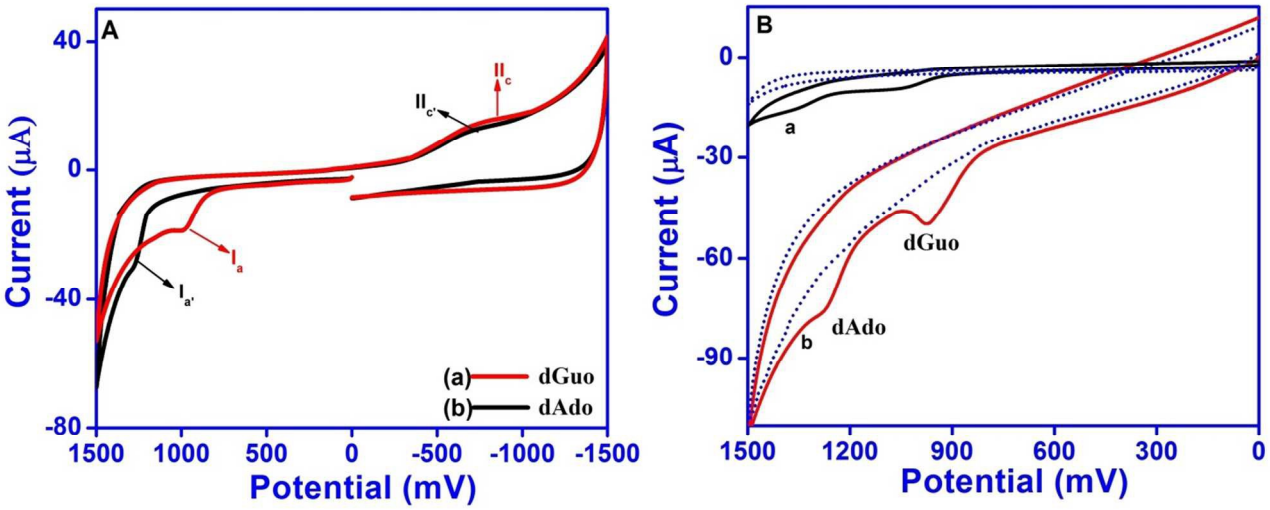

Fig. 4

RSC Advances Accepted Manuscript

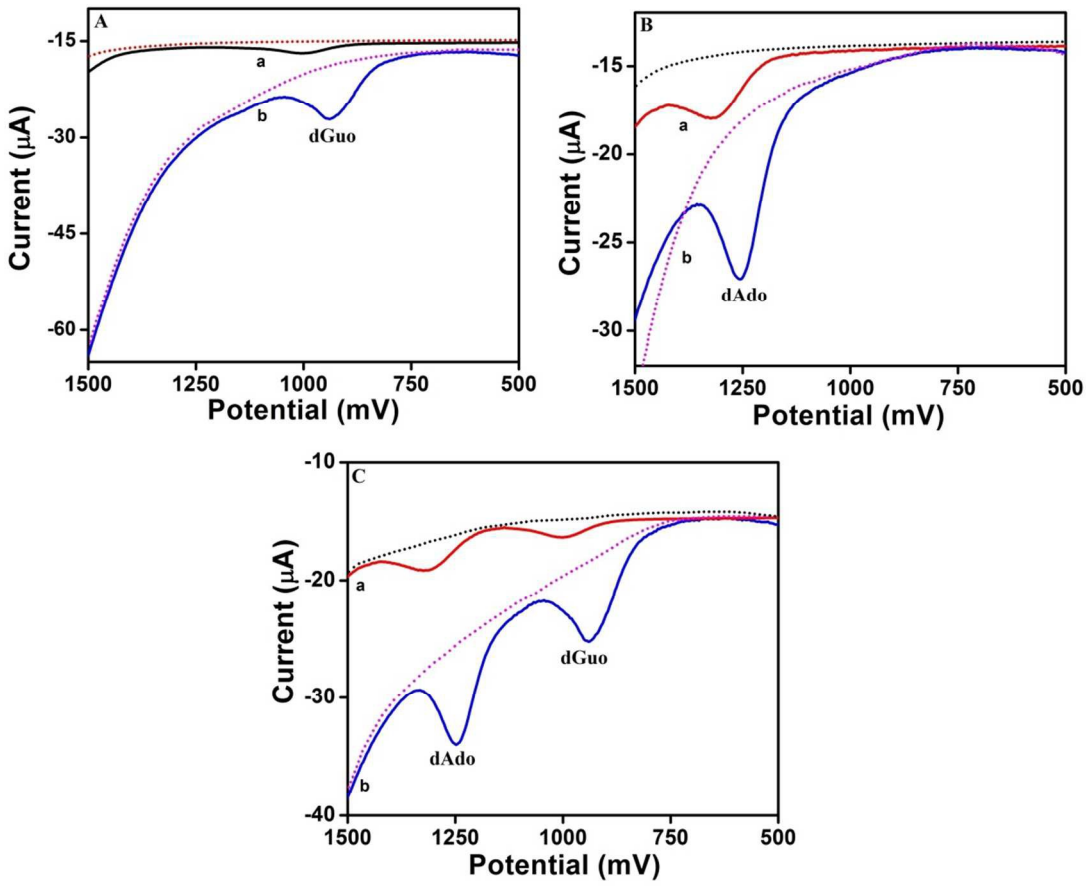

Fig. 5

RSC Advances Accepted Manuscript

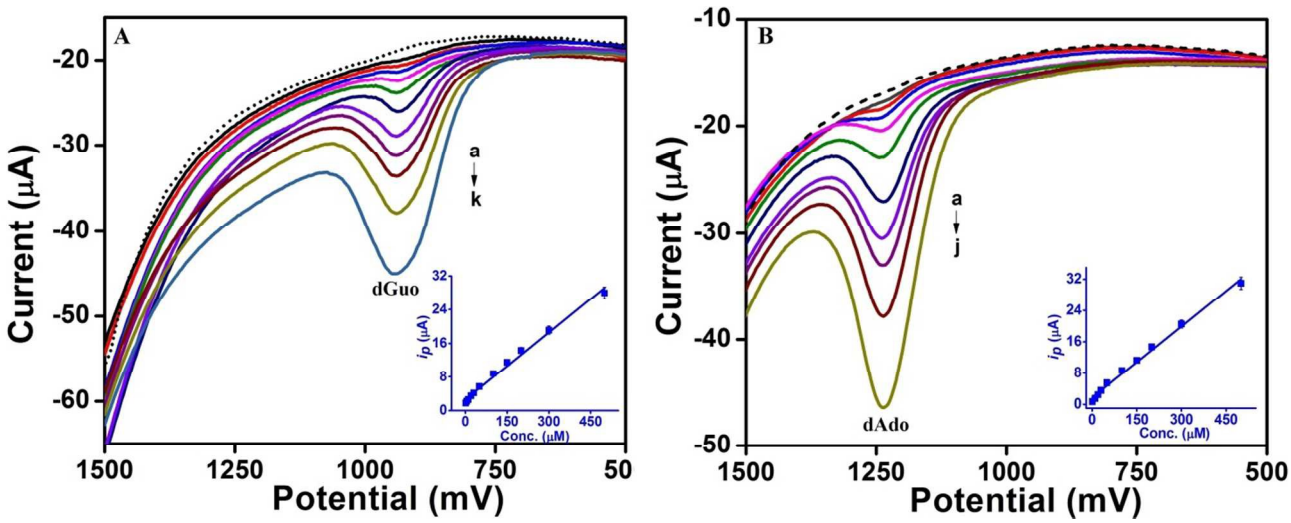

Fig. 6

RSC Advances Accepted Manuscript

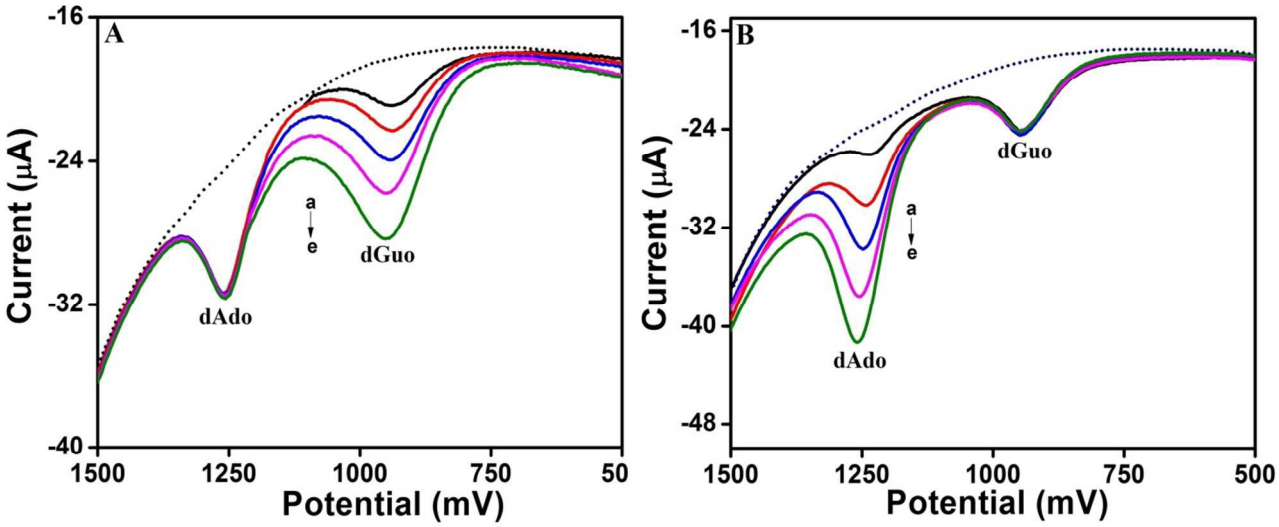

Fig. 7

RSC Advances Accepted Manuscript

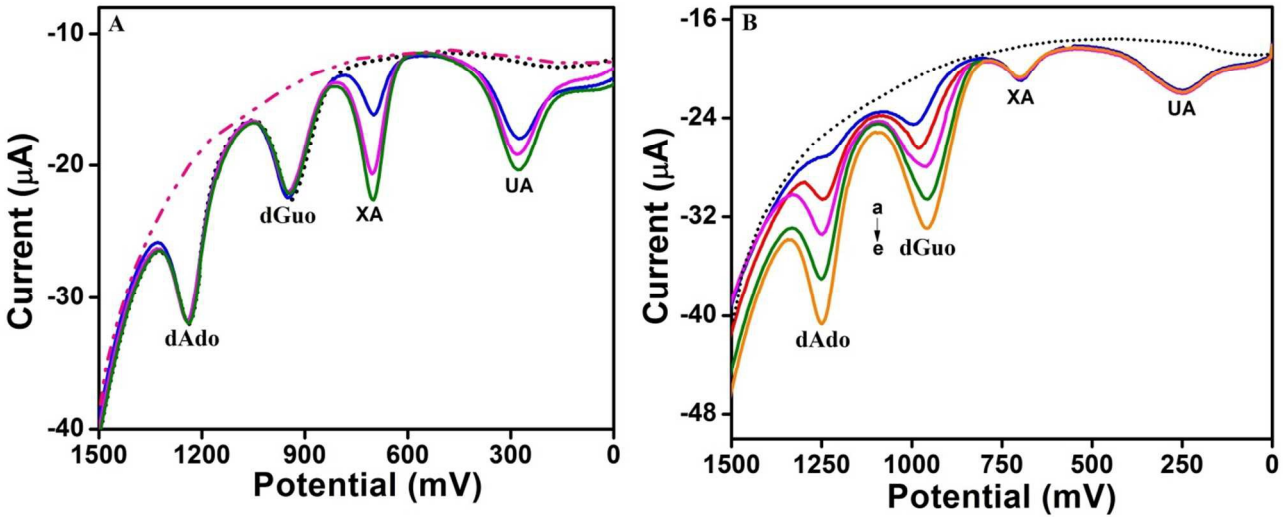

Fig. 8

RSC Advances Accepted Manuscript

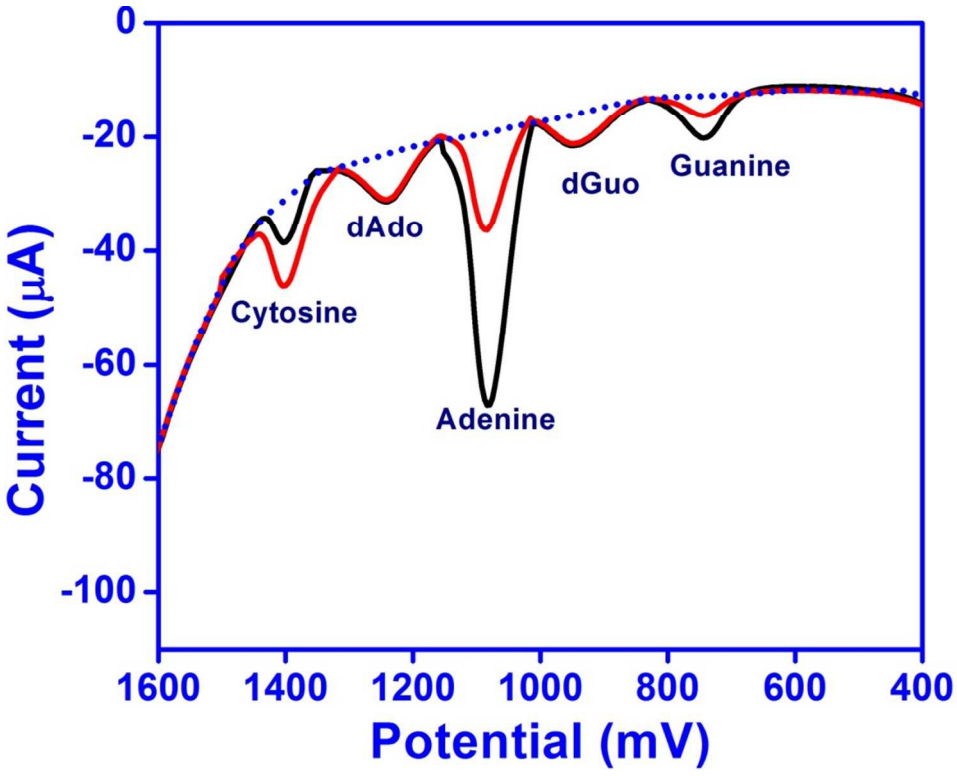

Fig 9

RSC Advances Accepted Manuscript

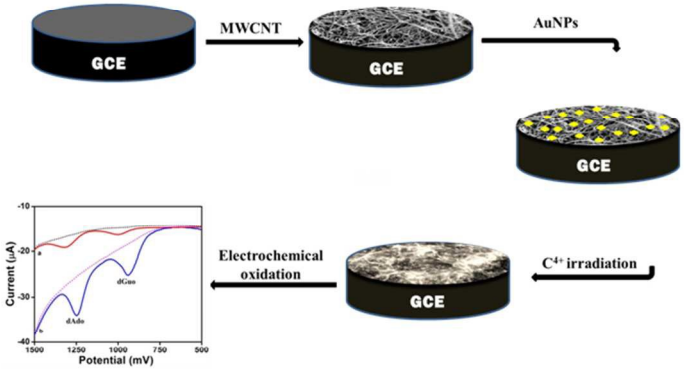

Sensor for purine nucleosides has been developed using irradiation with high energy carbon ion beam

254x190mm (96 x 96 DPI)

RSC Advances Accepted Manuscript